# Ultrastructural sonoporation bio-effects: Comparative study on two human cancer cell lines

Aya Zeghimi, Jean-Michel Escoffre, Ayache Bouakaz

10.1109/ULTSYM.2013.0016

# Ultrastructural sonoporation bio-effects: Comparative study on two human cancer cell lines

Aya Zeghimi, Jean-Michel Escoffre, Ayache Bouakaz
Inserm UMR-930 Imagerie & Cerveau,
Université François Rabelais Tours, France
aya.zeghimi@etu.univ-tours.fr

***Abstract*— Sonoporation increases transiently the cell membrane permeability, enabling the therapeutic compounds internalization into the cells. Several investigations reported heterogeneities in the permeabilization and transfection efficacy depending on the ultrasound (US) settings and cell type. Here, we compare the sonoporation effects on two human cell lines, glioblastoma and breast cancer using scanning electron microscopy (SEM). Adherent U-87 MG and MDA-MB-231 cells were insonated at 1 W/cm$^2$, during 60 s at 10% or 20% duty cycle, in the presence of BR14® microbubbles, added at a microbubble-cell ratio of 5. SYTOX® Green, a non-permeant fluorescent dye was used at 1µM, to quantify the membrane permeabilization using flow cytometry. The ultrastructural changes of the cell membrane morphology were monitored by SEM. Flow cytometry results show that the percentage of permeabilized U-87 MG cells reaches 60%, while this value doesn't exceed 40% for MDA-MB-231 cells. These results indicate that the percentage of permeabilized cells depends on the cell type. SEM observations were carried out to elucidate the differences in permeabilization rate between the two cell lines. The SEM analysis reveals that control cells show regular plasma membrane morphology. Their insonation in the presence of BR14® induce the formation of dark holes on their membrane surfaces (named here pore-like structures). However, the quantitative analysis of the SEM micrographs highlights noticeable differences in morphological changes post-sonoporation between the two cell lines. Thus, the mean number of pore-like structures is more abundant on U-87 MG cell membrane than on MDA-MB-231 cell membrane (645 vs. 290). In addition, the mean size of pore-like structures depends on the cell line. Indeed, the mean size on MDA-MB-231 cells was 40 ± 1.2 nm (30-60 nm) while this value reached 80 ± 0.9 nm (10 to 160 nm) for U-87 MG cells. In conclusion, the study confirms that the pore-like structures observed post sonoporation are directly associated to the cell permeabilization rate. Moreover, the observed differences in the permeabilization levels between both cell lines could be attributed to the differences in the number and size of pore-like structures that were seen on the cell membrane. This difference may be due to the fibroblastic nature of the U-87 MG cells in comparison to MDA-MB-231 cells.**

***Keywords*— *Sonoporation, U-87 MG, MDA-MB-231, Scanning electron microscopy , BR14® microbubbles.***

## I. Introduction

Sonoporation is a physical method based on the combination of ultrasound and microbubbles and induces an increase in the plasma membrane permeability. The increase in membrane permeability, leads to an uptake of therapeutic molecules. Several studies have attempted to define the exact bio-effect(s) and mechanism(s) of sonoporation. One of the hypothesized mechanisms is the formation of membrane pores [1–6] and a further stimulation of endocytosis pathways [7–10]. Otherwise, these studies are rather conflicting since none of them used the same experimental setup, or the same microbubbles.

The objective of this study is to highlight the ultrastructural sonoporation effects, on two different human cell lines (breast cancer and gliobstoma), using the same experimental setup (probe, microbubbles, etc). The morphological changes were explored by scanning electron microscopy.

## II. Material and Methods

### A. Cell Culture

Human glioblastoma cells (U-87 MG) and human breast cancer cells (MDA-MB-231) were seeded on 18 mm diameter glass cover slips, placed in 24 well-plates and containing Dulbecco's Modified Eagle's Medium (DMEM, Gibco-Invitrogen, Carlsbad, CA) supplemented with 10% v/v fetal calf serum (FCS, Gibco-Invitrogen, Carlsbad, CA) and incubated at 37°C under an humidified atmosphere in 5% $CO_2$ incubator. Cells were cultured until 80% confluence before ultrasound exposure.

### B. Ultrasound Exposure

Ultrasound waves were transmitted at 1MHz frequency (SoniGene™ systems, VisualSonics) for and 60 s at 1 W/cm², using a duty cycle of 10%, 20% for MDA-MB-231 and U-87 MG, respectively. Ultrasound contrast agent, BR14® (Bracco Research, Switzerland) was added into the well at a microbubble/cell ratio of 5. These acoustic parameters were obtained as a result of prior optimization experiments.

### C. Cell Permeabilization

SYTOX® Green, a small and non-permeant molecule was used, at a final concentration of 1 µM, to monitor the membrane permeabilization, by flow cytometry. Immediately after sonoporation, the cell medium was removed and the cells were washed with Phosphate Buffered Saline (PBS, Gibco-Invitrogen, Carlsbad, CA) and collected through centrifugation (4 min, 800 g). The cells were resuspended in

500 µL of PBS. The cell mortality was assessed by flow cytometry after propidium iodide staining (0.5 µg/mL). Fluorescence histograms were recorded with a flow cytometer (Beckman-Coulter, Fullerton, CA) and analyzed using the Kaluza software supplied by the manufacturer. A minimum of 10 000 events were analyzed to generate each histogram. The gate was arbitrarily set for the detection of red and green fluorescence. The ultrasound conditions described earlier were reproduced to measure the rate of SYTOX® Green uptake in the cells.

### *D. Scanning Electron Microscopy (SEM)*

The ultrastructural modifications of the cells, after sonoporation, were monitored by SEM. The sonoporated cells were attached by immersion in 2% paraformaldehyde and 1% glutaraldehyde based fixative at room temperature. Cells were fixed at different post-sonoporation time points, either immediately (0 min) or 15 min post-sonoporation.
Ten cells per condition were included in the analysis (n=10).

## III. Results and Discussion

### *A. Cell membrane permeabilization*

The SYTOX® Green incorporation is an indicator of membrane permeability. Flow cytometry results show different membrane permeabilization rates, for both cell lines, at the selected ultrasound conditions and in combination with BR14® microbubbles. While U-87 MG membrane permeabilization rate reached 60%, the SYTOX® Green incorporation in MDA-MB-231 cells did not exceed 48.1 ± 0.2 % (Figure 1). Cell mortality did not exceed 2% for both cell lines (data not shown). This difference could be due to the migratory capacity of the MDA-MB-231 cells, which makes more difficult the activity of the commonly used transfection agents [11].

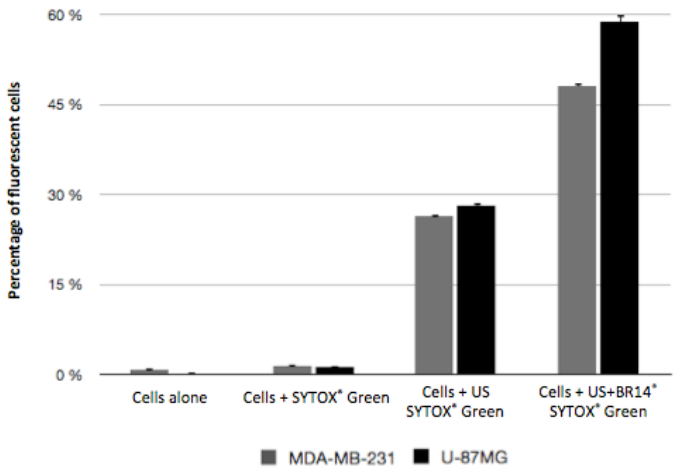


**Figure 1:** Percentage of the SYTOX® Green incorporation expressed in percentage of fluorescent cells, in U-87 MG and MDA-MB-231 cells. Data are shown as mean ± SD.

### *B. Scanning eletron microscopy observations*

Based on the SEM photomicrographs control cells (No US), for both cell lines, show regular plasma membrane morphology, while insonified cells, at the same US parameters, exhibit dark spots (Figure 2). These spots are termer here pore-like structures.

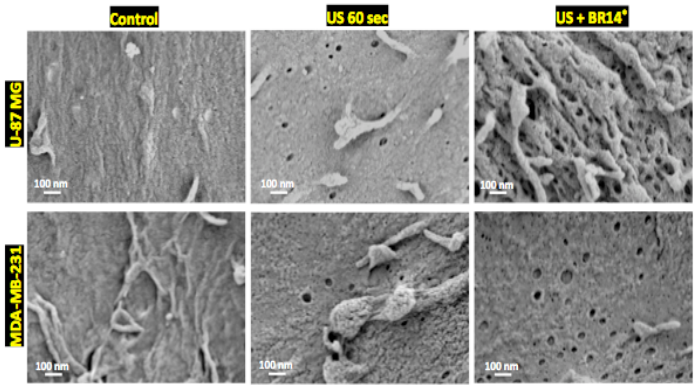


**Figure 2:** SEM photomicrographs showing the morphology of the U-87 MG and MDA-MB-231plasma membrane, at 50 000 time magnification for three conditions (control cell, ultrasound alone, and ultrasound+BR14® microbubbles). Scale bar 100 nm.

These microscopic observations show also that BR14® microbubbles enhance the appearance of pore-like structures at the plasma membrane for both cell lines (U-87 MG and MDA-MB-231). However, there are some notable differences in morphological changes post-sonoporation between the two cell lines. MDA-MB-231 cells have less pore-like structures compared to U-87 MG cells. The quantitative study confirms these observations (Figure 3). Indeed, the pore-like structures present at the membrane level are more abundant for U-87 MG (645 pore-like structures), against 290 pore-like structures for MDA-MB-231. These results may explain the observed difference in the rate of membrane permeabilization between MDA-MB-231 and U-87 MG.

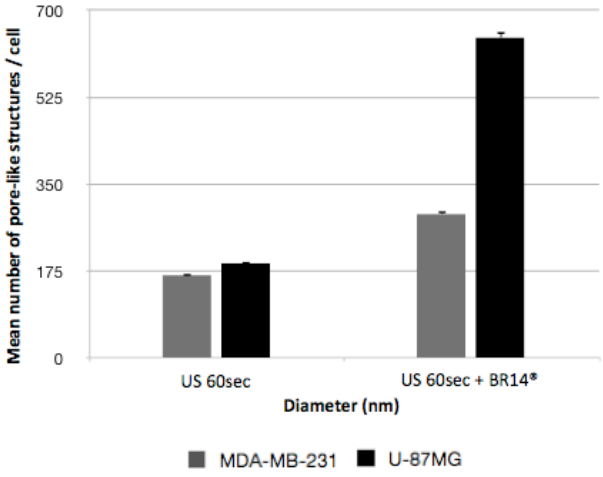


**Figure 3:** The mean number of pore-like structures per cell, for two conditions (US alone, and US + BR14® microbubbles). 10 analyzed cells per condition. Data are shown as mean ± SD.

The size and the number of the pore-like structures were measured for both cell lines. This quantitative study (Figure 4) shows that the mean size of the pore-like structures on MDA-MB-231 cells is 40 ± 1.2 nm (30-60 nm) while this value reaches 80 ± 0.9 nm (10 to 160 nm) for U-87 MG cells. One can appreciate also that the pore-like structures with a mean

size between 30 and 60 nm are more abundant on the U-87 MG cell membrane. This result suggests that the mean size of the pore-like structures depends on the cell line.

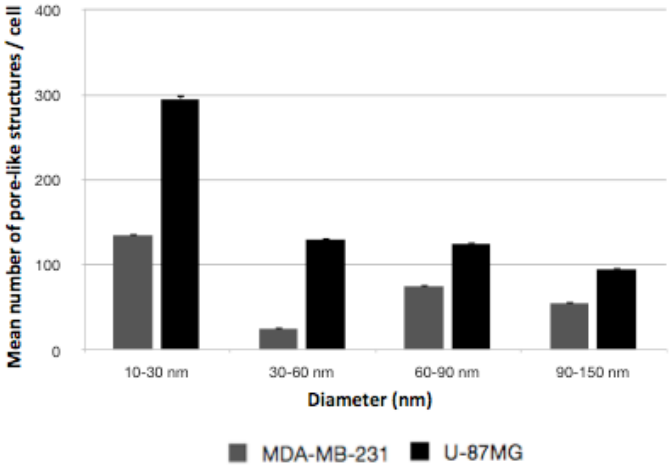


**Figure 4:** Mean number of pore-like structures versus the diameter, for the two cell lines (MDA-MB-231 and U-87 MG).

This difference in the sonoporation rate between the two studied cell lines could be attributed to their cellular structures [1], suggesting that U-87 MG cells are more sensitive than MDA-MB-231 to the sonoporation. Indeed, since these two cell lines are considered as epithelial cells, U-87 MG unlike MDA-MB-231 tend to be fibroblastic.

Furthermore, the cells were attached and observed 15 min post-sonoporation. The SEM images show that both cell types exhibit less pore-like structures on the membranes, indicating that the cells remain active, and resorb these membrane disruptions. In addition, the counting confirms a decrease in the pore-like structures number, for both MDA-MB-231 and U-87 MG cells (Figure 5). However, this decrease is more pronounced for MDA-MB-231, since approximately 80% of pore-like structures disappeared 15 min only after sonoporation. For the U-87 MG cells, the number of pore-like structures decayed by about 40% only 15 min post-sonoporation.

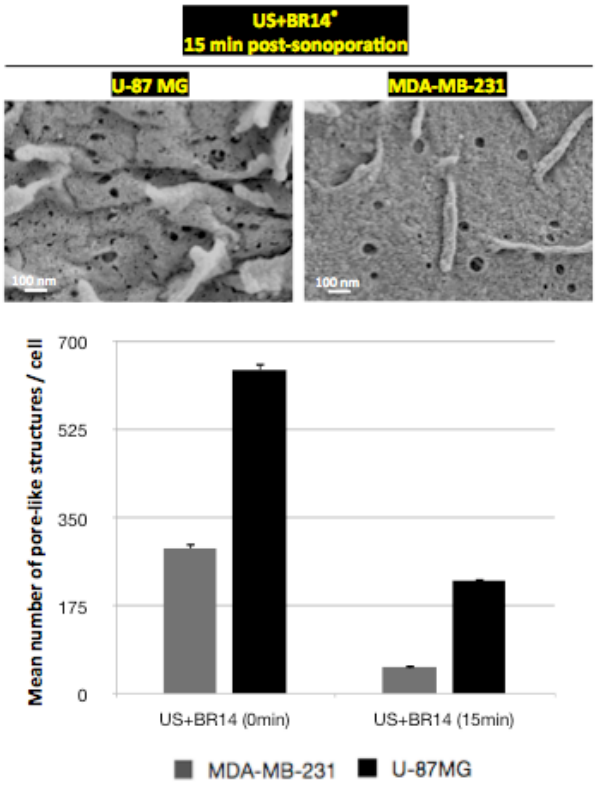


**Figure 5:** Upper panel shows SEM images of MDA-MB-231 and U-87 MG 15 min post-sonoporation. Lower panel depicts the counting of pore-like structures on the plasma membrane of cells, 15 min post-sonoporation.

## IV. Conclusions

This study confirms that the pore-like structures observed post-sonoporation are directly associated to the cell permeabilization level, for both cell lines. The electron microscopy observations confirm the heterogeneity between cell lines, in response to sonoporation. In addition, the morphological differences between this two cell lines (MDA-MB-231 and U-87 MG) and especially the fibroblastic nature of the U-87 MG cells may explain the difference in sonoporation rates between both cell lines.

## Acknowledgments

We thank D. Rustem Uzbekov and Claude Lebos for their technical assistance. The authors are grateful to Bracco Research Geneva, for supplying the Microbubbles. The authors also thank Visualsonics©, for lending the Vevo® SoniGene™ sonoporator. The EU Project SONODRUGS (NMP4-LA-2008-213706) funded this project.

## References

[1] M. L. Andrew A. Brayman, S. Coppage, and M. W. M. Vaidya, "Transient poration and cell surface receptor removal from human lymphocytes in vitro by 1 MHz ultrasound" *Ultrasound in medicine & biology*, vol. 25, no. 6, pp. 999 –1008, 1999.

[2] M. J. K. Blomley, J. C. Cooke, E. C. Unger, M. J. Monaghan, and D. O. Cosgrove, "Science, medicine, and the future: Microbubble contrast agents : a new era in ultrasound." *British Medical Journal*, vol. 322, no. 7296, pp. 1222-25, 2001.

[3] P. Prentice, A. Cuschieri, K. Dholakia, M. Prausnitz, and P. Campbell, "Membrane disruption by optically controlled microbubble cavitation," *Nature Physics*, vol. 1, no. 2, pp. 107–110, 2005.

[4] A. Zeghimi, R. Uzbekov, B. Arbeille, J.M. Escoffre, A. Bouakaz, "Ultrastructural modifications of cell membranes and organelles induced by sonoporation," IEEE International Ultrasonics Symposium Proceedings. Germany, pp. 2045-48, October 2012 [*IEEE International Ultrasonics Symposium*, Dresden, Germany, Oct. 2012].

[5] R. Schlicher, H. Radhakrishna, T. Tolentino, R. Apkarian, V. Zarnitsyn, and M. Prausnitz, "Mechanism of intracellular delivery by acoustic cavitation," *Ultrasound in medicine & biology*, vol. 32, no. 6, pp. 915–924, 2006.

[6] I. Lentacker, B. Geers, J. Demeester, S. C. De Smedt, and N. N. Sanders, "Design and evaluation of doxorubicin-containing microbubbles for ultrasound-triggered doxorubicin delivery: cytotoxicity and mechanisms involved," *Molecular therapy*, vol. 18, no. 1, pp. 101–8, 2010.

[7] L. J. M. Juffermans, A. van Dijk, C. a M. Jongenelen, B. Drukarch, A. Reijerkerk, H. E. de Vries, O. Kamp, and R. J. P. Musters, "Ultrasound and microbubble-induced intra- and intercellular bioeffects in primary endothelial cells," *Ultrasound in medicine & biology*, vol. 35, no. 11, pp. 1917–27, 2009.

[8] V. Lionetti, A. Fittipaldi, S. Agostini, M. Giacca, F. a. Recchia, and E. Picano, "Enhanced Caveolae-Mediated Endocytosis by Diagnostic Ultrasound In Vitro," *Ultrasound in Medicine & Biology*, vol. 35, no. 1, pp. 136–143, 2009.

[9] B. D. M. Meijering, L. J. M. Juffermans, A. van Wamel, R. H. Henning, I. S. Zuhorn, M. Emmer, A. M. G. Versteilen, W. J. Paulus, W. H. van Gilst, K. Kooiman, N. de Jong, R. J. P. Musters, L. E. Deelman, and O. Kamp, "Ultrasound and microbubble-targeted delivery of macromolecules is regulated by induction of endocytosis and pore formation," *Circulation research*, vol. 104, no. 5, pp. 679–87, 2009.

[10] D. M. B. Paula, V. B. Valero-Lapchik, E. J. Paredes-Gamero, and S. W. Han, "Therapeutic ultrasound promotes plasmid DNA uptake by clathrin-mediated endocytosis.," *The journal of gene medicine*, vol. 13, no. 7–8, pp. 392–401, 2011.

[11] Y. Wang, C.Y. Ke, C. Weijie Beh, S.Q. Liu, S.H. Goh, and Y.Y. Yang, "The self-assembly of biodegradable cationic polymer micelles as vectors for gene transfection.," *Biomaterials*, Vol. 28, no. 35, pp. 5358-68, 2007.